1.7 Some Theoretical Consequences of the FT Method

When analyzing the scan data of an object, collected as shown in Figure 2.3.2, it is practical to work with a new coordinate system x_1', x_2' that is rotated together with the transmitter and receiver:

$$\begin{cases} x_1' = x_1 \cos\theta + x_2 \sin\theta \\ x_2' = -x_1 \sin\theta + x_2 \cos\theta \end{cases}, \quad \begin{cases} x_1 = x_1' \cos\theta - x_2' \sin\theta \\ x_2 = x_1' \sin\theta + x_2' \cos\theta \end{cases}, \qquad (1\ \text{a,b})$$

or in matrix notation

$$\begin{bmatrix} x_1' \\ x_2' \end{bmatrix} = \begin{bmatrix} & U & \end{bmatrix} \begin{bmatrix} x_1 \\ x_2 \end{bmatrix}$$

where the matrix $U = \begin{bmatrix} \cos\theta & \sin\theta \\ -\sin\theta & \cos\theta \end{bmatrix}$ is orthogonal (i.e. $U^T U = I$). Hence

$$\begin{bmatrix} x_1 \\ x_2 \end{bmatrix} = \begin{bmatrix} & U & \end{bmatrix}^T \begin{bmatrix} x_1' \\ x_2' \end{bmatrix}$$

Figure 1 illustrates this change of variables, as well as a corresponding one for Fourier space.

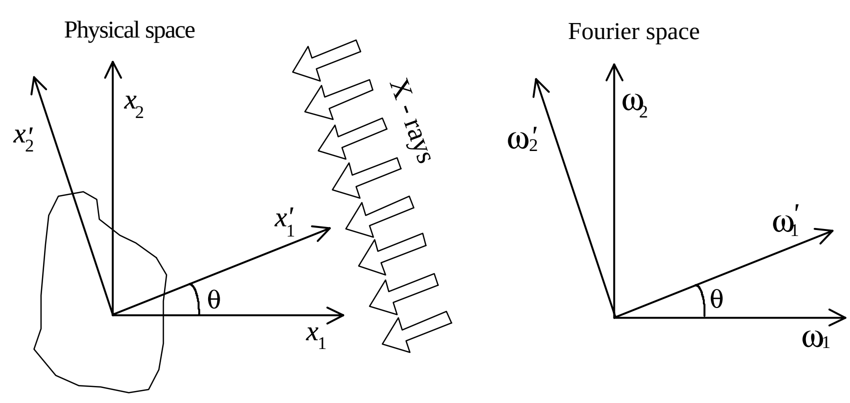

Figure 1 a,b. Original and rotated coordinate systems in physical- and Fourier space (Part a matches Figure 1.3-4).

When $\theta = 0$, the two physical-space systems agree. For each angle $0 \le \theta < \pi$, the scan data can be written

$$g(x_2', \theta) = \int_{-\infty}^{\infty} f(x_1, x_2)\, dx_1' \ . \tag{2}$$

Immediate back projection, as shown in Figure 1.5-2, gives

$$h(x_1, x_2) = \int_0^{\pi} g(x_2', \theta)\, d\theta \tag{3}$$

(note here that for x_1, x_2 given, x_2' becomes a function of θ). This function $h(x_1, x_2)$ for our model problem was shown in Figure 1.5-3. It amounts to a 'smeared' approximation of the original object, represented by the function $f(x_1, x_2)$. In the following two subsections, we will see how the FT method tells how to modify the integrand in (3) so that the result becomes exact (i.e. equal to $f(x_1,x_2)$ instead of $h(x_1,x_2)$). The two verssions below are mathematically equivalent:

1. replace $g(x_2',\theta)$ by $\displaystyle\int_{-\infty}^{\infty} \left[\int_{-\infty}^{\infty} g(x_2', \theta)\, e^{-i\omega_2' x_2'}\, dx_2' \right] |\omega_2'|\, e^{i\omega_2' x_2'}\, d\omega_2$, and

2. replace $g(x_2',\theta)$ by $\displaystyle\frac{1}{2\pi^2} \int_{-\infty}^{\infty} \frac{\partial g(\xi, \theta)/\partial \xi}{x_2' - \xi}\, d\xi$.

Case (1), derived next, leads again to the BP method - and provides analytically the form of the filter to use. We then also derive Case (2), which is Radon's original closed-form inversion formula. This latter version is mathematically elegant, but is numerically inappropriate, both because its derivative and its principal value integral.

1.7.1 FT Method Cast as a BP Procedure

We showed in section 1.6.1 that the FT method provided an exact reconstruction of the original object. This fact forms the key ingredient in the following argument:

$$f(x_1, x_2) = \int_{-\infty}^{\infty}\int_{-\infty}^{\infty} \hat{f}(\omega_1, \omega_2)\, e^{i\omega_1 x_1 + i\omega_2 x_2}\, d\omega_1\, d\omega_2 =$$

Inverse double Fourier transform; change the double integral into polar coordinates: $\omega_1 = -\rho \sin\theta$, $\omega_2 = \rho\cos\theta$; $\frac{d(\omega_1,\omega_2)}{d(\rho,\theta)} = \rho$.

$$= \int_0^{2\pi}\int_0^{\infty} \hat{f}(\rho, \theta)\, e^{-i\rho\sin\theta\, x_1 + i\rho\cos\theta\, x_2}\, \rho\, d\rho\, d\theta =$$

Change notation from ρ to ω_2' and alter the description of the domain from $0 \le \rho < \infty, 0 \le \theta \le 2\pi$ to $-\infty < \omega_2' < \infty$, $0 \le \theta \le \pi$.

$$= \int_0^{\pi} \int_{-\infty}^{\infty} \hat{f}(\omega_2', \theta)\ e^{i\,\omega_2' x_2'}\ |\omega_2'|\ d\omega_2'\ d\theta =$$

Now use the key result of the FT method;
$\hat{f}(\omega_2', \theta) = \frac{1}{2\pi} \int_{-\infty}^{\infty} g(x_2', \theta)\ e^{-i\,\omega_2' x_2'}\ dx_2'$.

$$= \frac{1}{2\pi} \int_0^{\pi} \left\{ \int_{-\infty}^{\infty} \left[\int_{-\infty}^{\infty} g(x_2', \theta)\ e^{-i\,\omega_2' x_2'}\ dx_2' \right] |\omega_2'|\ e^{i\,\omega_2' x_2'}\ d\omega_2 \right\} d\theta \quad .$$

Comparing this with (3), we see that immediate back projection would have offered an exact reconstruction, had we modified the integrand $g(x_2', \theta)$ to

$$\int_{-\infty}^{\infty} \left[\int_{-\infty}^{\infty} g(x_2', \theta)\ e^{-i\,\omega_2' x_2'}\ dx_2' \right] |\omega_2'|\ e^{i\,\omega_2' x_2'}\ d\omega_2' \qquad (4)$$

(we are ignoring multiplicative factors). A modification such as this is known as a *convolution*, described in Table 1, Section II.2.3-2. Implemented in physical space, we would need to find a function (in physical space) whose Fourier transform is equal to $|\omega|$. Convolving the scan data with this function would cause filtered back projection to become exact. We will next try to find this function and, in particular, see if it bears any resemblance to the discrete function 0, 0, ... , 0, -0.4, 1.0 , -0.4, 0, ... , 0, 0 that we found experimentally to work so well (in Section 1.5).

When using the BP approach, we can apply (4), as it stands, to each scan function $g(x_2', \theta)$. However, this would cost two FFTs per function (scan line). A computationally much cheaper approach is to use the insight from (4) to devise a BP filter, i.e. to find the physical-space filter which, in Fourier space, corresponds to a multiplication with $|\omega_2'|$. In simplified notation, we are looking for a function $f(x)$ that has the Fourier transform $|\omega|$, i.e.

$$|\omega| = \frac{1}{2\pi} \int_{-\infty}^{\infty} f(x)\, e^{-i\,\omega x}\ dx$$

or

$$f(x) = \int_{-\infty}^{\infty} |\omega|\, e^{i\,\omega x}\ d\omega \qquad . \qquad (5)$$

This attempt runs into a road block - the integral (5) is divergent.

A simple way to gain insights into what $f(x)$ would 'look like' (if it existed) is to discretize (5) and look for the discrete Fourier transform of a function $|\omega|$ (for finite number of points N, the sum corresponding to (5) has to be finite - the pattern as $N \to \infty$ will reveal what (5) could not). We assuming the DFT code we are using has its frequencies ordered the 'natural' way (as in the code fftc rather than fft in the code sections ?? and ?? resp.):

Frequency:	$(-\frac{N}{2}+1),\ (-\frac{N}{2}+2),\ \ldots,-2,-1,\ 0,\ 1,\ 2,\ \ldots(\frac{N}{2}-2),\ (\frac{N}{2}-1)$													
Enter value:	$(\frac{N}{2}-1),\quad (\frac{N}{2}-2),\quad \ldots,\ 2,\ \ 1,\ 0,\ 1,\ 2,\ \ldots(\frac{N}{2}-2),\ (\frac{N}{2}-1)$.													

After having normalized the FFT output by multiplying it with $4\,/\,N^2$, we get

$N=$ 32	....	-.0176	0.0	-.0464	0.0	-.4066	1.0000	-.4066	0.0	-.0464	0.0	-.0176	....	
$N=$ 64	....	-.0165	0.0	-.0454	0.0	-.4056	1.0000	-.4056	0.0	-.0454	0.0	-.0165	....	
$N=128$	....	-.0163	0.0	-.0451	0.0	-.4054	1.0000	-.4054	0.0	-.0451	0.0	-.0163	....	
......														
limit $N\to\infty$	....	-.0162	0.0	-.0450	0.0	-.4053	1.0000	-.4053	0.0	-.0450	0.0	-.0162	....	=
=	....	$-\left(\frac{2}{5\cdot\pi}\right)^2$	0.0	$-\left(\frac{2}{3\cdot\pi}\right)^2$	0.0	$-\left(\frac{2}{1\cdot\pi}\right)^2$	1.0	$-\left(\frac{2}{1\cdot\pi}\right)^2$	0.0	$-\left(\frac{2}{3\cdot\pi}\right)^2$	0.0	$-\left(\frac{2}{5\cdot\pi}\right)^2$	....	

The center three entries

-.4053 1.0000 -.4053

very much dominate the other entries. We have arrived at the same type of filter as was empirically proposed in equation (1.5-2) and also to the value $\beta \approx 0.4$ that was found there to be near-optimal.

1.7.2 Derivation of Radon's inversion formula

Our first attempt to analyze the FT-BP link failed when the integral in (5) turned out to be divergent. Although the numerical approximation of the integral proved so successful, let us return once more to the analysis, but now focus on (4) instead. In simplified notation, the key result here is

$$\int_{-\infty}^{\infty}\left[\int_{-\infty}^{\infty} g(\xi)\, e^{-i\,\omega\xi}\, d\xi\right]|\omega|\, e^{i\,\omega x}\, d\omega = \frac{1}{\pi}\int_{-\infty}^{\infty}\frac{d\,g(\xi)/d\,\xi}{x-\xi}\, d\xi \qquad (6)$$

<u>Derivation of (6):</u> Assuming both the scan data g(ξ) and its Fourier transform decay sufficiently fast to make all the integrals below convergent, equation (6) can be shown as follows:

Note that the LHS of (6) is the (inverse - Fourier-to-physical) transform of the function

$$\left[\int_{-\infty}^{\infty} g(\xi)\, e^{-i\,\omega\xi}\, d\xi\right]\cdot|\omega| \quad . \qquad (7)$$

We can then establish (6) by

i. rewriting the RHS of (6) (using in the first step integration by parts):

$$\int_{-\infty}^{\infty}\frac{d\,g(\xi)/d\,\xi}{x-\xi}\, d\xi = -\int_{-\infty}^{\infty} g(\xi)\, d\left(\frac{1}{x-\xi}\right) = -\int_{-\infty}^{\infty}\frac{g(\xi)}{(x-\xi)^2}\, d\xi = \frac{d}{dx}\int_{-\infty}^{\infty}\frac{g(\xi)}{x-\xi}\, d\xi \qquad (8)$$

and

ii. showing that its Fourier transform agrees with (7):

$$\int_{-\infty}^{\infty}\left[\frac{1}{\pi}\frac{d}{dx}\int_{-\infty}^{\infty}\frac{g(\xi)}{x-\xi}d\xi\right]e^{-i\omega x}dx =$$

Integrate by parts

$$= \frac{i\omega}{\pi}\int_{-\infty}^{\infty}\int_{-\infty}^{\infty}\frac{g(\xi)}{x-\xi}d\xi\, e^{-i\omega x}dx =$$

Swap order of integration

$$= \frac{i\omega}{\pi}\int_{-\infty}^{\infty}g(\xi)\left[\int_{-\infty}^{\infty}\frac{e^{-i\omega(x-\xi)}}{x-\xi}dx\right]e^{-i\omega\xi}d\xi$$

Set $x-\xi=t$; the inner (principal value) integral then evaluates as $\int_{-\infty}^{\infty}\frac{\cos\omega t}{t}dt - i\int_{-\infty}^{\infty}\frac{\sin\omega t}{t}dt =$ $0 - i\pi\times\left\{\begin{array}{c}1 \text{ if } \omega>0\\ -1 \text{ if } \omega<0\end{array}\right\} = -i\pi\frac{|\omega|}{\omega}$.

$$=\left[\int_{-\infty}^{\infty}g(\xi)\,e^{-i\omega\xi}d\xi\right]\cdot|\omega|$$

This identically matches (7).

The analytical procedure of applying the RHS of (6) to the scan data before performing the back projection can now be summarized as follows:

<u>Radon transform theorem:</u>

Let $g(x_2', \theta) = \int_{-\infty}^{\infty} f(x_1, x_2)\, dx_1'$ be a path integral of a function $f(x_1,x_2)$ along the ray x_2'= constant (forming the angle θ to the x_1-axis). Then $f(x_1,x_2)$ can be recovered through

$$f(x_1, x_2) = \frac{1}{2\pi^2}\int_0^{\pi}\int_{-\infty}^{\infty}\frac{\partial g(\xi,\theta)/\partial\xi}{x_2' - \xi}\, d\xi\, d\theta \qquad . \qquad (9)$$

This inversion formula is analytically exact, mathematically elegant but - as mentioned above - numerically impractical.

1.7.3 Example of application of Radon's formula

We noted in Section 1.5.3 - and verified by direct integration - that back projecting from all angles with the scan data

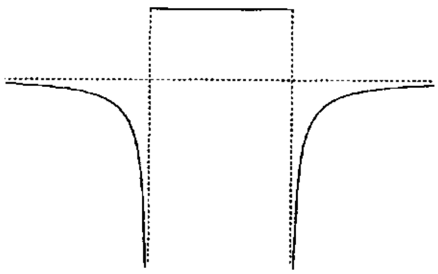

$$k(r) = \begin{cases} 1 & |r| \le 1 \\ 1 - \frac{|r|}{\sqrt{r^2-1}} & |r| > 1 \end{cases} \qquad (10)$$

produced a circular constant-intensity object on a zero background. With Radon's result, we can derive this function $k(r)$ in (10) as follows:

True scan data of a circular cylinder of unit radius (same for all angles) becomes

$$g(\xi) = \begin{cases} \sqrt{1-\xi^2} & |\xi| \le 1 \\ 0 & |\xi| > 1 \end{cases} .$$

To achieve an exact reconstruction under back projection, this function must be modified according to (6). Writing (6) in the form of the last part of (8), we get

$$k(r) = \frac{1}{\pi}\frac{d}{dr}\int_{-1}^{1}\frac{\sqrt{1-\xi^2}}{r-\xi}d\xi = \frac{d}{dr}\begin{cases} r & |r| \le 1 \\ r - sign(r)\sqrt{r^2-1} & |r| > 1 \end{cases} =$$

$$= \begin{cases} 1 & |r| \le 1 \\ 1 - \frac{|r|}{\sqrt{r^2-1}} & |r| > 1 \end{cases} .$$

1.7.4 Compact summary of FT-derivation

Given a density function $f(x_1,x_2)$, a detector measures

$$g(x_2', \theta) = \int_{-\infty}^{\infty} f(x_1, x_2)\, dx_1 \qquad \text{(cf. equation 2)}$$

For a point on the x_2'-axis (see Figure 1 a,b, or set $x_1' = 0$ in eq. (1b))

$$\begin{cases} x_1 = -x_2' \sin\theta \\ x_2 = \quad x_2' \cos\theta \end{cases} \quad . \qquad (11)$$

Multiplication by $\sin\theta$ and $\cos\theta$ resp., and adding gives

$$x_2' = -x_1 \sin\theta + x_2 \cos\theta \quad .$$

We next determine the Fourier transform of our desired density function

$$\hat{f}(\omega_1, \omega_2) = \frac{1}{(2\pi)^2} \int_{-\infty}^{\infty} \int_{-\infty}^{\infty} f(x_1, x_2)\, e^{-i(\omega_1 \cdot x_1 + \omega_2 \cdot x_2)}\, dx_1\, dx_2 \quad . \qquad (12)$$

Along the line $\omega_1' = 0$, we find (in analogy with (11))

$$\begin{cases} \omega_1 = -\omega_2' \sin\theta \\ \omega_2 = \quad \omega_2' \cos\theta \end{cases} \quad .$$

Hence, the integral in (12) becomes

$$\hat{f}(\omega_1, \omega_2) = \frac{1}{(2\pi)^2} \int_{-\infty}^{\infty} \int_{-\infty}^{\infty} f(x_1, x_2)\, e^{-i(\omega_2' \sin\theta \cdot x_1 + \omega_2' \cos\theta \cdot x_2)}\, dx_1\, dx_2 =$$

$$= \frac{1}{(2\pi)^2} \int_{-\infty}^{\infty} \int_{-\infty}^{\infty} f(x_1, x_2)\, e^{-i\, \omega_2' (-x_1 \sin\theta + x_2 \cos\theta)}\, dx_1\, dx_2 =$$

Note: i. $(-x_1 \sin\theta + x_2 \cos\theta) = x_2'$,
ii. coordinate change dx_1, dx_2 to dx_1', dx_2' has Jacobian = 1

$$= \frac{1}{(2\pi)^2} \int_{-\infty}^{\infty} \left[\int_{-\infty}^{\infty} f(x_1, x_2)\, dx_1' \right] e^{-i\, \omega_2' x_2'}\, dx_2' = \frac{1}{(2\pi)^2} \int_{-\infty}^{\infty} g(x_2', \theta)\, e^{-i\, \omega_2' x_2'}\, dx_2' =$$

$$= \frac{1}{2\pi}\, \hat{g}(\omega_2', \theta) \, .$$

This establishes the complete FT-method (as shown in Figure 1.6-2).